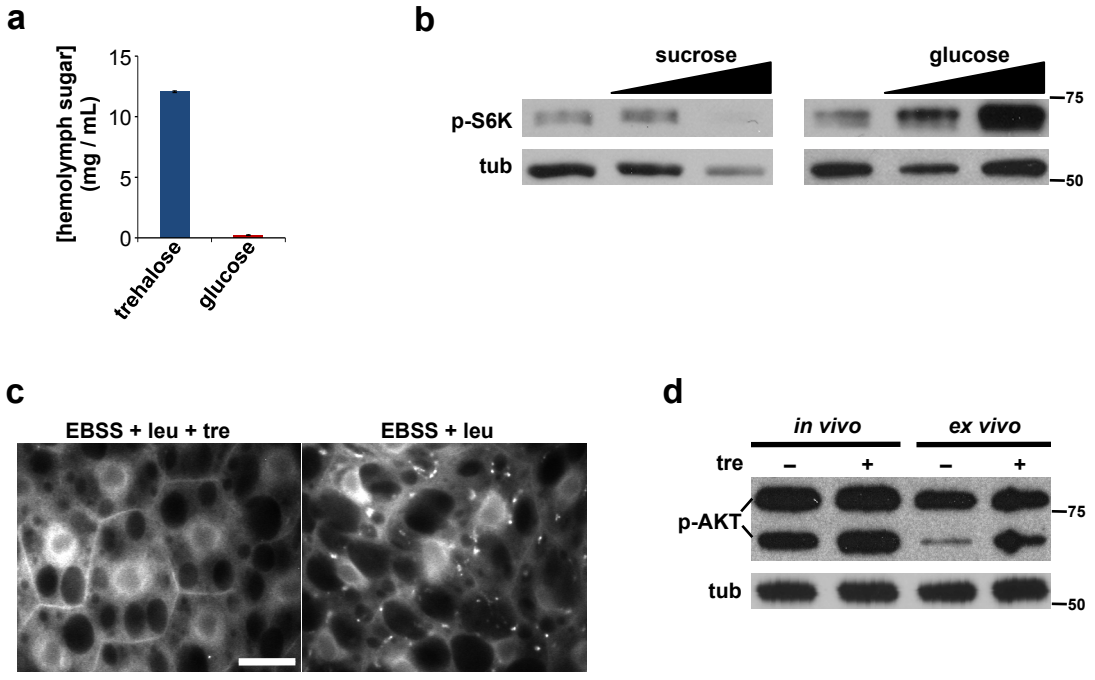

Supplementary Figure 1: Alternative *ex vivo* conditions and assays for fat body TOR activity. **(a**) *In vivo* levels of circulating trehalose and glucose in third instar larvae. **(b)** *Ex vivo* phosphorylation of S6K T398 in response to increasing concentration of sucrose or glucose (0, 20 or 40 mg/ml in M3 medium). **(c)** Accumulation of mCherry-Atg8a punctae after 4 hrs *ex vivo* incubation in EBSS/leucine medium with (left) and without (right) 20 mg/ml trehalose. Scale bar 20 µm. **(d)** Phosphorylation of AKT S505 is stimulated by trehalose *in vivo* (26.6 mg/ml in agar/ tryptone food) and *ex vivo* (40 mg/ml in M3 medium). Data in a, b, and d each represent three independent experiments. Images in c are representative of two trials each using seven carcasses per condition. Full size immunoblots are presented in Supplementary Figure 6.

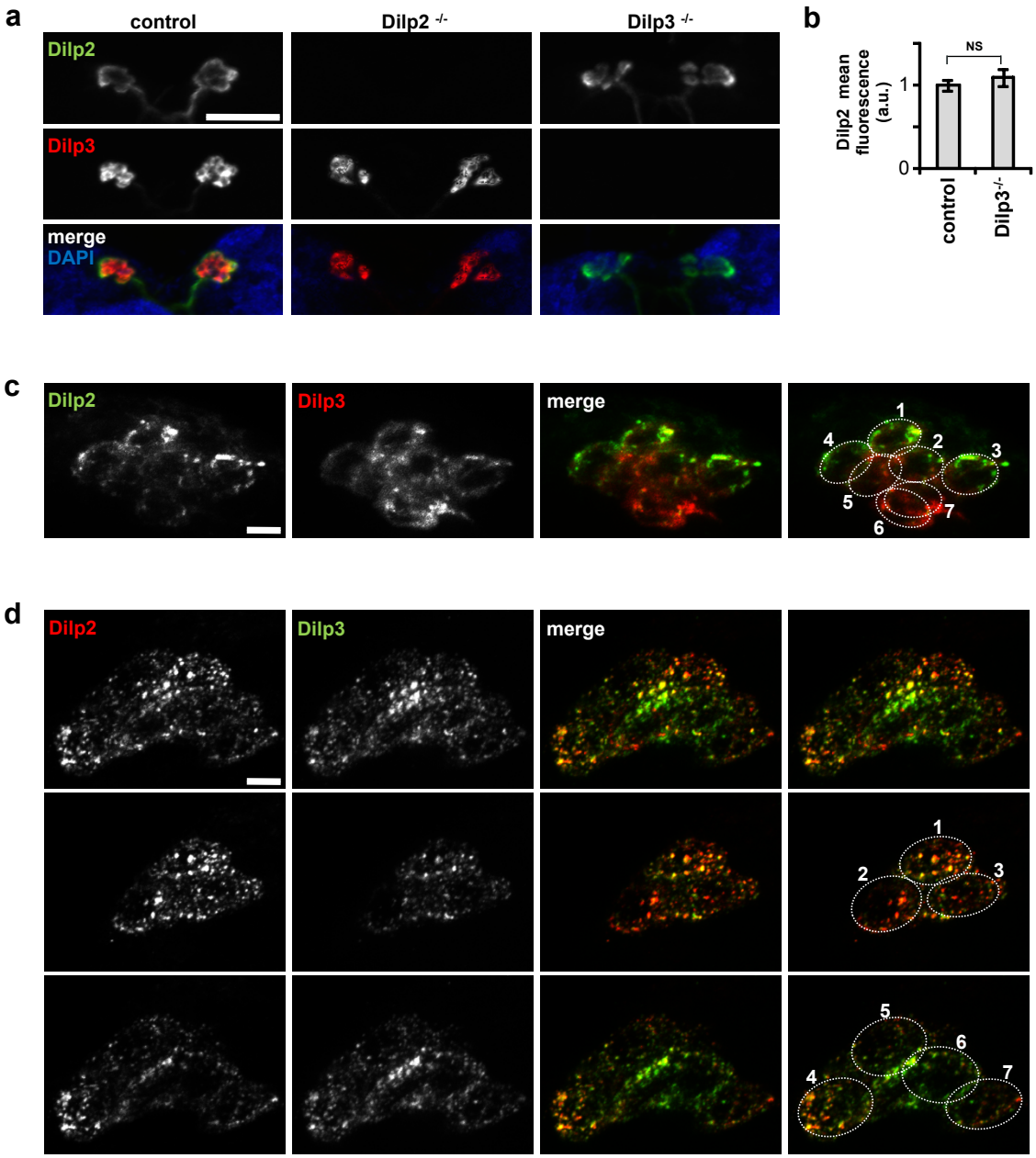

Supplementary Figure 2: Antibody controls. **(a, b)** Specificity of Dilp antibodies. Anti-Dilp2 labels the IPCs in control and *Dilp3*$^{-/-}$ but not *Dilp2*$^{-/-}$ larvae. Anti-Dilp3 labels the IPCs in control and *Dilp2*$^{-/-}$ but not *Dilp3*$^{-/-}$ larvae. Dilp2 fluorescence intensity is not significantly different between control and *Dilp3*$^{-/-}$ IPCs. Data represent mean±s.e.m., n=11. NS: P>0.05, student's t-test. **(c)** Additional confocal image showing distinct patterns of Dilp2 and Dilp3 localization in IPCs (rabbit anti-Dilp2, mouse anti-Dilp3 as in Figure 4) following 4 hr complete starvation. **(d)** Combined Z-stack (top) and individual (middle, bottom) confocal sections of Dilp2- and Dilp3-stained IPCs, using independently-derived 1° antibodies from those shown in Figures 4 and S2C (rat anti-Dilp2, Texas Red anti-rat; rabbit anti-Dilp3, FITC anti-rabbit). Scale bars 50 µm (a), 5 um (c, d). Images in c and d are each representative of two independent experiments, n=7.

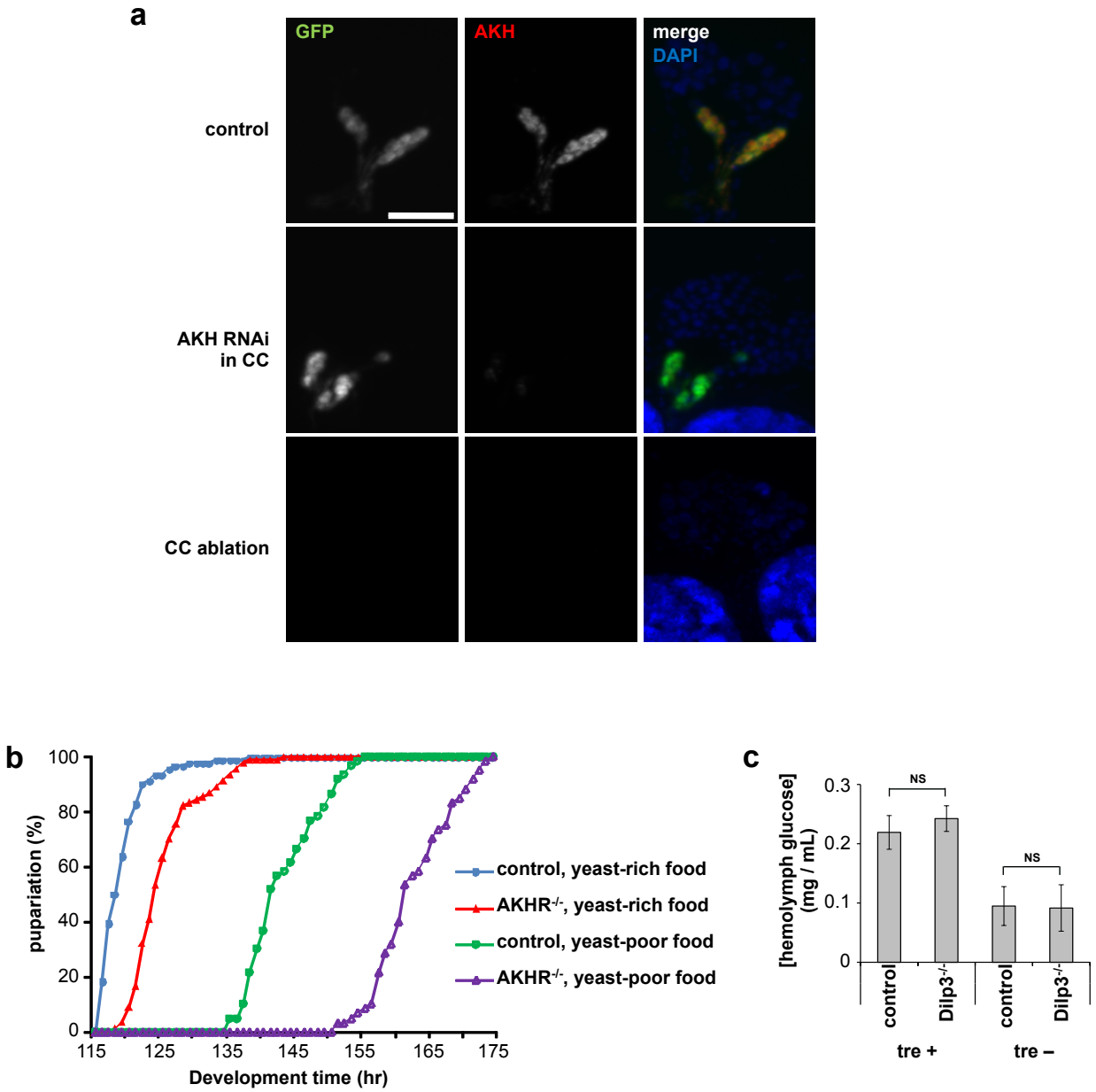

Supplementary Figure 3: AKH signaling controls and effects. **(a)** Efficiency of AKH depletion and corpora cardiaca ablation. Anti-AKH staining reveals robust loss of AKH protein in CC cells expressing AKH dsRNA (middle; *AKH-GAL4 UAS-GFP / UAS-AKH^{RNAi})* and loss of the CC by targeted expression of reaper (bottom; *AKH-GAL4 UAS-GFP / UAS-reaper)*. Scale bar 50 µm. Representative images of seven larvae per genotype are shown. **(b)** Developmental timing measurements of *AKHR* null mutant and matched controls raised on rich and poor media (standard fly food with and without supplemental yeast, respectively). Data are from three vials of 30 larvae for each experimental condition. **(c)** Levels of circulating glucose in control and *Dilp3$^{-/-}$* larvae cultured in the presence or absence of trehalose *in vivo*. Data represent mean±s.e.m. of three independent experiments. NS: P>0.05, student's t-test.

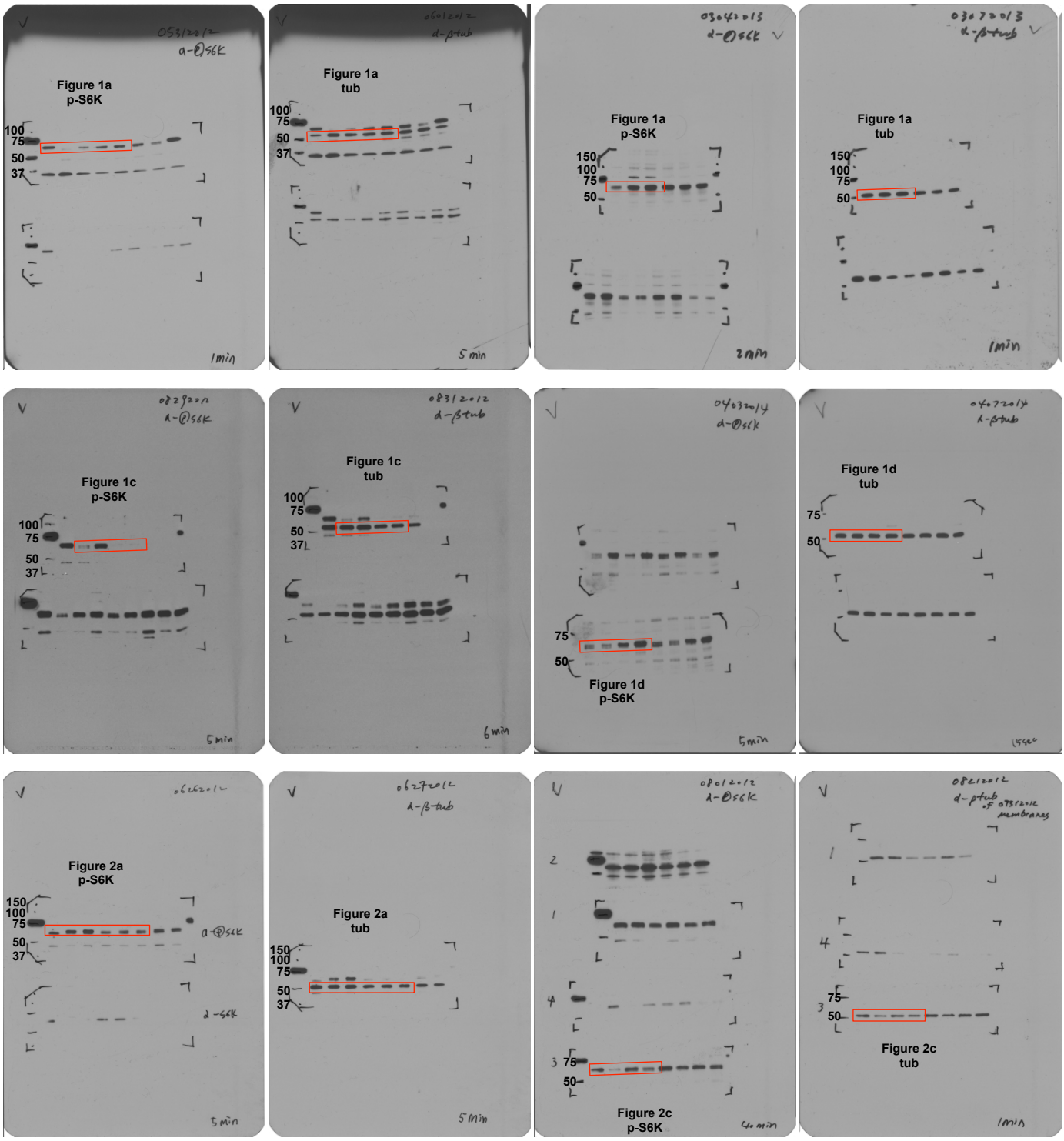

Supplementary Figure 4: Whole gel scans of immunoblots presented in Figures 1 and 2.

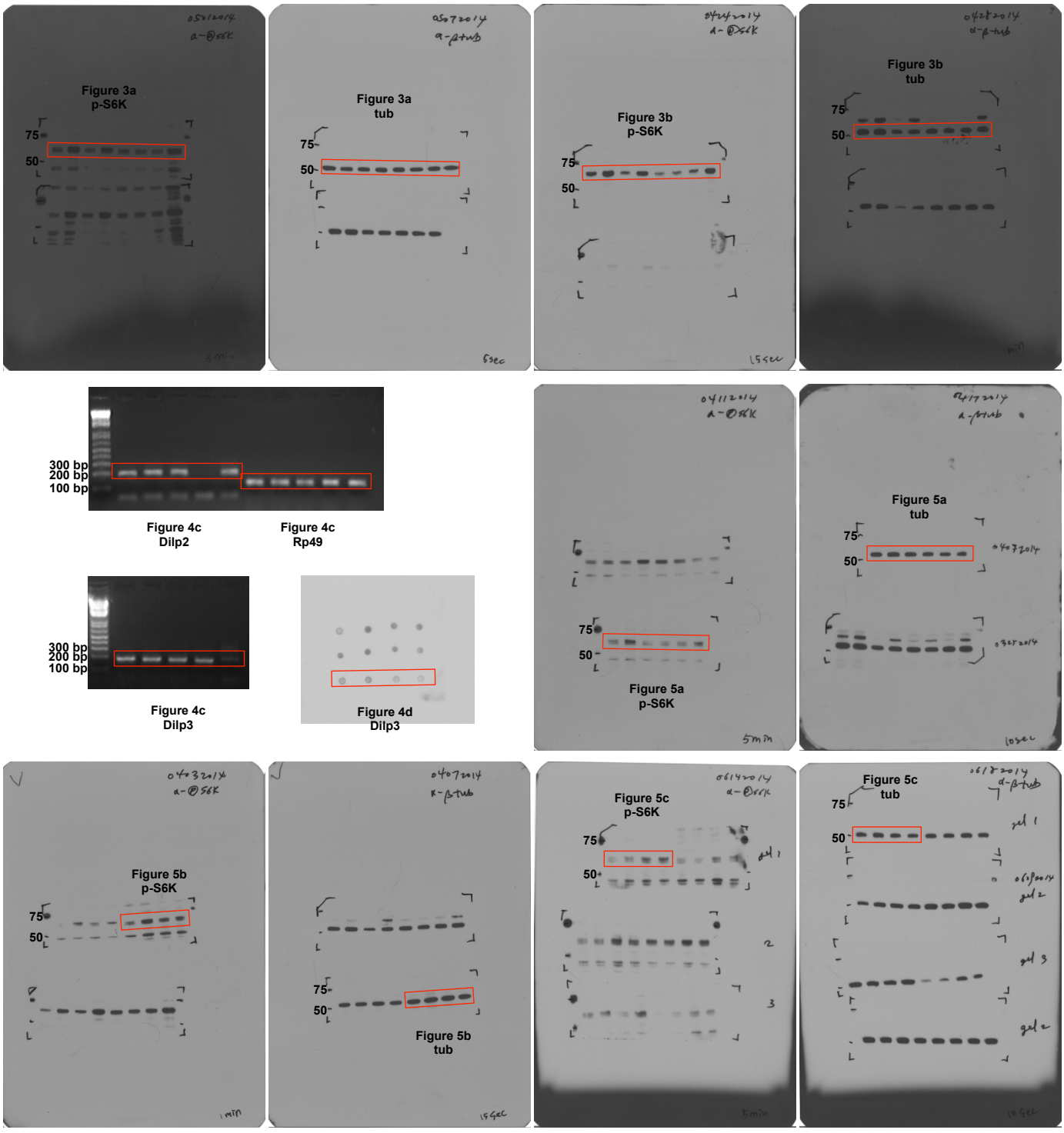

Supplementary Figure 5: Whole gel scans of immunoblots and gels presented in Figures 3, 4 and 5.

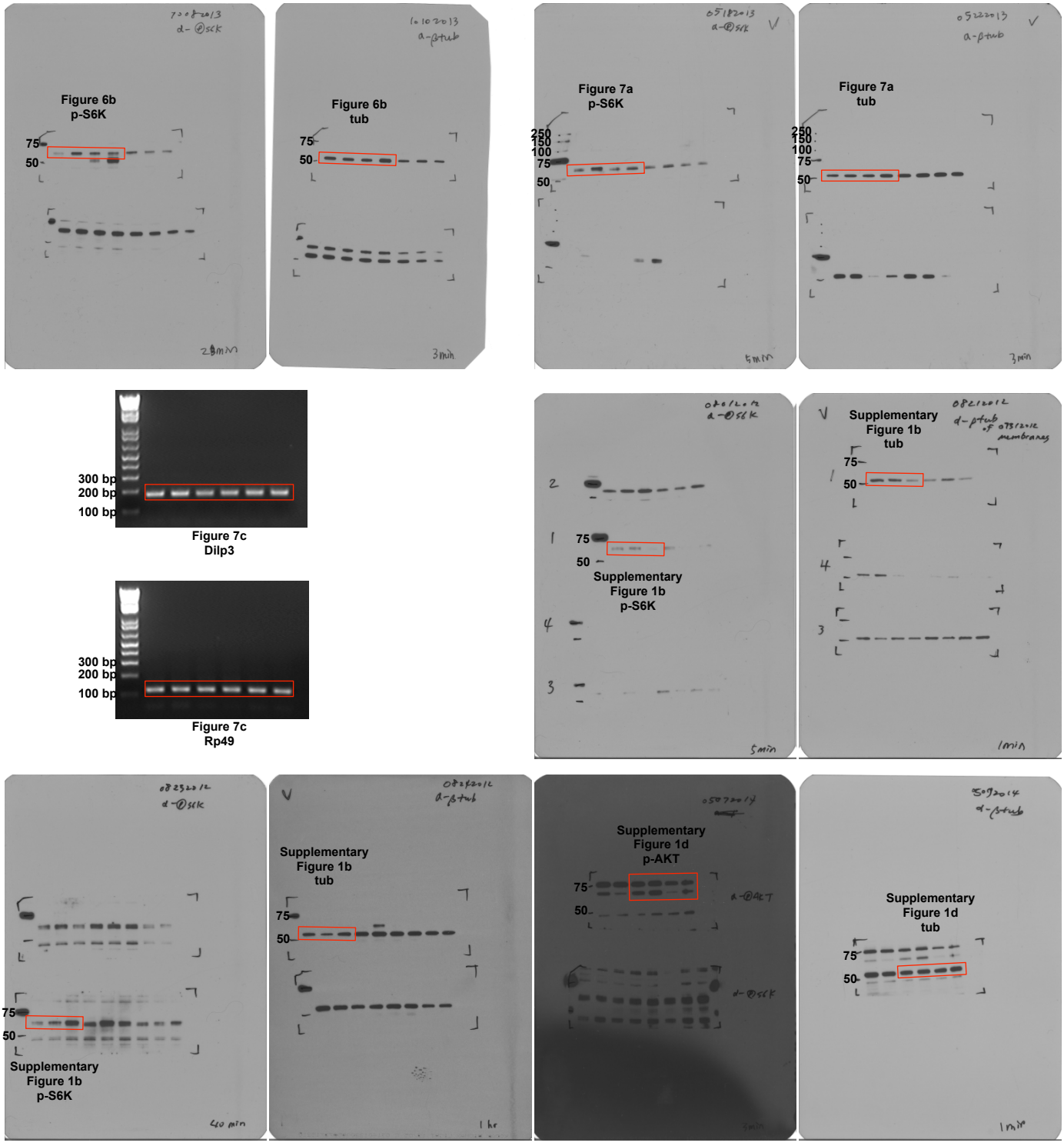

Supplementary Figure 6: Whole gel scans of immunoblots and gels presented in Figures 6, 7, and Supplementary Fig. 1.